第3卷 第1期　　航空动力学报　　Vol.3 No.1
1988年1月　　Joural of Aerospace Power　　Jan. 1988

轮盘热光弹性研究

沈阳航空发动机研究所　董本涵　王举

摘　要

本文叙述了轮盘热光弹性试验的三个主要方面的工作：(1)轮盘模型热负荷的施加方法及模型温度场的测量与记录方法；(2)进行平面轮盘模型试验与理论计算结果比较，以考核试验方法；(3)进行某发动机涡轮盘的模型试验，得到稳定温度场下的热应力分布。

热光弹性法是用光弹性进行热应力的模拟试验。1975年 Berger 在其“热模拟”[1]一文中对此做了全面总结。由于相似条件比较苛刻以及实验技术上的困难，热光弹性试验真正解决具体工程问题还不太多。但是要在原型上直接测量热应力也困难重重，且不经济。所以对发动机涡轮盘等热负荷较大的零件进行模型试验仍有价值。本文总结了热光弹性试验中热负荷的模拟、温度场测量等方面的研究成果。并给出了平面盘热应力考核试验的结果，试验结果与理论计算比较符合。作者还进行了某发动机涡轮盘在给定稳定温度场下的热应力试验，得到了较完整的热应力数据，尤其是关于涡轮盘榫槽、偏心孔处的热应力集中资料，更是其他方法难以得到的。

一、热光弹性试验方法

进行热光弹性模型试验模拟原型的热应力分布时，必须保证热传导相似，即热传导方程相同、边值条件相似、边值条件构成的相似准则相等。模拟稳定温度场的热应力试验不必考虑初始条件，仅需满足边值条件相似即可。稳定温度场的实现采用第一类边界条件相似比较容易实现，即保证模型表面温度T_{bm}分布与原型表面温度T_b分布相似。为了保证试验精度，还需保证模型材料在试验温度范围内其光学性质、机械性质不变，还要有一定的灵敏度。本试验中选用环氧树脂材料为模型材料。

1. **模型热负荷施加方案及温度测量方法**　为保证模型表面温度分布与原型表面温度分布相似，在模型表面涂炭膜，根据温度分布曲线形状将炭膜分成相应的小段，每小段两端粘接铜片以连接交直流电源，通过改变炭膜厚度及小段两端的电压来控制各段炭膜的加热量，在炭膜外表面用毡子与空气绝热。在各段炭膜与模型表面之间埋设热电偶（必须与炭膜绝缘），此热电偶及加热导线与动圈表连接。动圈表将根据热电偶输入的温度信号及预先给定的温度值控制加热电流的输出，从而达到边界温度的自动控制。模型表面及内部的温度场用埋设镍铬-考铜热电偶并通过自动记录仪测量。

2. **应力测量方法**　模型热应力测量方法与传统光弹性法相同，将具有温度分布的模型置于偏振光场中，即可观察到与模型热应力的主应力差及主应力方向有关的等色线和等倾线，利用光弹性仪可以精确地测量模型内的等色线条纹级序和等倾线值，据此可以分离出热

本文于1987年4月收到。

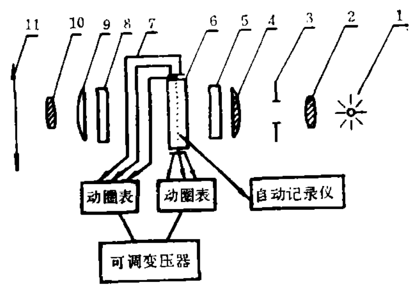

图 1 实验装置简图（1.光源，2.聚光镜，3.光栏，4.准直镜，5.起偏镜及1/4波片，6.模型，7.电源线，8.1/4波片及分析镜，9.视场镜，10.投影物镜，11.屏幕）

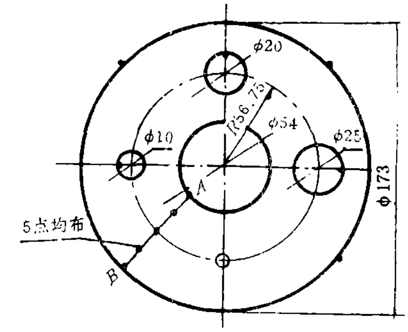

图 2 带偏心孔平面盘热电偶测温点位置图（δ = 8）

应力值，应力分离方法也可采用常规的方法（本文采用剪力差法)。试验装置见图 1

为了考核本试验方法的可靠性，进行了有理论解的平面盘的热光弹性试验。平面盘模型及热电偶测温点位置见图 2，轮盘外缘表面温度为$T_1 = 67℃$，中心孔及偏心孔表面温度为$T_3 = 17℃$，侧面温度T_2相当空气温度。由试验得到的中心孔及偏心孔边的热应力(Q_θ)分布图 3)。Q_θ指切于模型边界的应力。用剪应力差法〔2〕分离AB截面（见图 2）上的应力σ_t周向应力)、σ_r（径向应力),并与按文献〔3〕计算的结果比较（图 4)。由图 4 可见，本试验结果与计算结果比较吻合，故本试验可适用于工程试验。

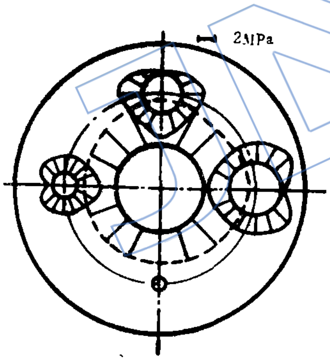

图 3 平面盘中心孔偏心孔孔边应力σ_θ分布

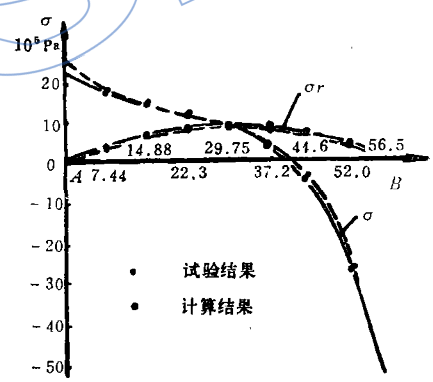

图 4 AB截面应力分布(试验结果与计算结果比较)

二、涡轮盘热光弹性试验

图5A所示为某发动机涡轮盘结构及壁温分布。为了测定该涡轮盘的热应力，先将实际结构简化为图 5B所示的力学模型，其温度场也做了一定的简化。实际结构的温度为T，周围气体温度为$T_气$。力学模型的温度为T',模型周围气体温度为$T'_气$。力学模型的温度场按图5B分布，则保证了模型轮盘腹板及轮缘部分的温度场与原型分布相似。

进行热光弹性试验时，在模型盘外缘施加热负荷的方法是将炭膜预先涂在聚酯薄膜上，用201油膏粘贴于模型表面,炭膜沿圆周等分 8 段，每段电阻为$2k\Omega \sim 5k\Omega$，各段炭膜端电压

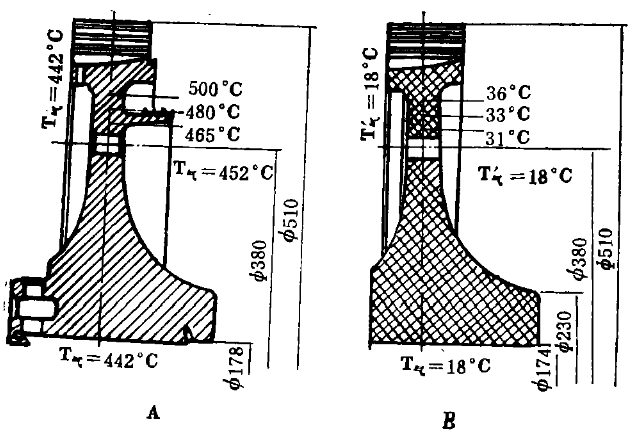

图 5　涡轮盘结构A和力学模型B及温度场

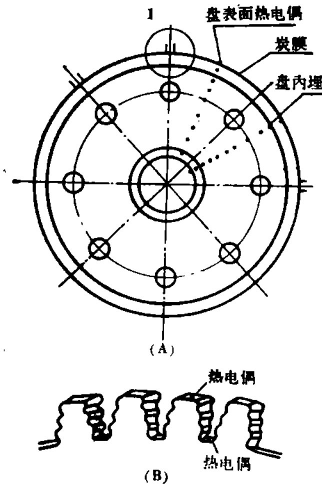

图 6　模型炭膜及热电偶位置

为150 V。由动圈表自动控温。调节轮盘的轮缘温度场，使所得的轮盘沿半径方向的温度分布如图5B所示，并保证温度稳定不变。炭膜测温热电偶位置见图 6 。

试验结果

1.　盘腹板处等倾线及主应力迹线（见图 7 ）；

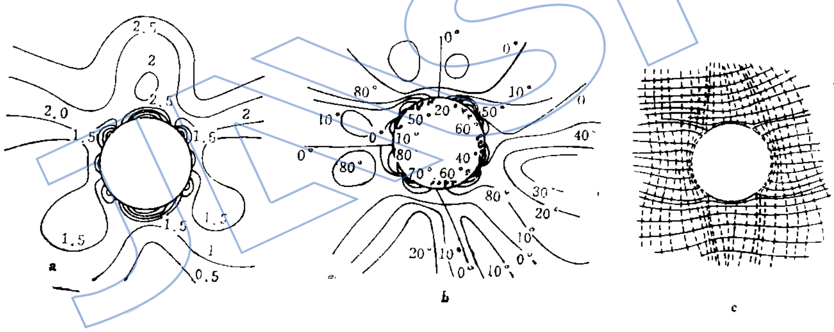

图 7　腹板及偏心孔描绘等色线 (a) 等倾线 (b) 主应力迹线(c)

2.　偏心孔孔边应力σ_θ及槽底应力σ_C分布（图 8 ）（σ_θ、σ_C 均为切于自由边界的应力）

3.　a-a、b-b截面的应力分布（图 9 ，图10）

根据热弹性相似条件可以由模型热应力换算出原型应力（本文给出的应力数据为模型应力数据），换算公式为：

$$\sigma_{ij} = (E/E_m)\cdot(\alpha/\alpha_m)\cdot G\cdot\sigma^m_{ij}$$

其中E、E_m为原型、模型材料弹性模数，α、α_m为原型、模型材料热膨胀系数，$G=\Delta T/\Delta T_m$ ΔT、ΔT_m为原型、模型温差。

由涡轮盘的热光弹性试验结果可知，在盘的偏心孔边由于热流集中，所以存在较大应力集中，榫槽底部也存在较高应力水平。本试验是模拟发动机开车条件下稳定温度场引起的涡轮盘热应力试验。用本方法可以模拟涡轮盘在不同温度场下的热应力分布。

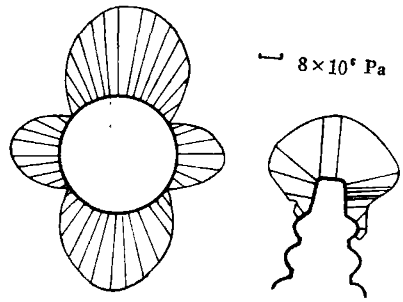

图 8　偏心孔周边界应力σ_θ及榫槽边界应力σ_c分布

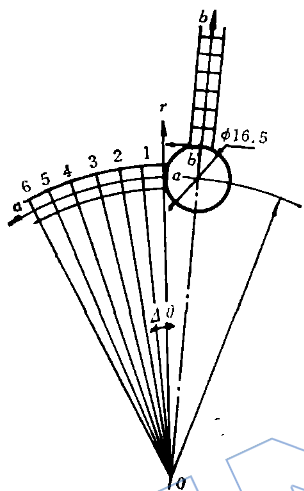

图 9　轮盘周向截面a-a，径向截面b-b的位置

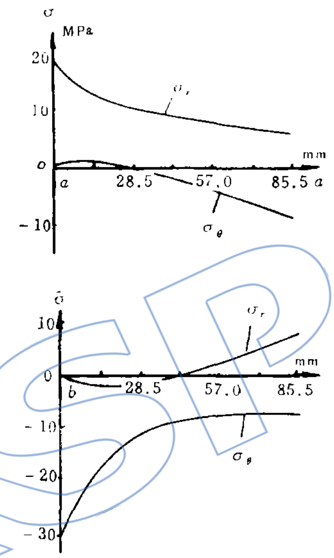

图10　模型沿截面a-a，b-b的应力分布（σ_r—径向应力σ_θ—周向应力）

参 考 文 献

〔1〕 Weibet, E.E.,Proc. of 5th International Conference Application Mechanics, p213.1939.
〔2〕 航空发动机强度设计手册，第二篇，第一章，112页。
〔3〕 航空发动机强度设计手册，第二篇，第三章，10页。

（责任编辑　李其汉）

We found that the scheme can be stable in any case if the relaxation coefficient is greater than one. For calculation of boundary layers over blade surfaces, an integral method which can treat turbulent separating flows is studied. The coupling method of inviscid flow with boundary layer flow is also given in this paper. Several computed results of transonic flows in cascades show good agreement with experimental data. It is anticipated that this analysis system will provide a useful tool for engineering design.

INVESTIGATION ON STEADY-STATE RESPONSE OF A ROTOR-SUPPORT SYSTEM WITH TWO SQUEEZE-FILM DAMPERS

Li Xifan and Fu Caigao

(*Gas Turbine Establishment*)

Abstract

The rotor investigated is supported on two major ball bearings with squeeze-film dampers in the absence of the centralizing retaining springs. The coefficients of the film forces are linearized by using dynamical performances of the damper in the fixed coordinate system (four oil-film stiffness and four oil-film damping coefficients). The steady-state unbalance responses of an asymmtrical flexile rotor system has been easily determined by means of transfer matrix and linear iterative methods. Generally speaking, for the rotor system with nonlinear squeeze-film dampers, the optimum damper design with suitable unbalance level of the rotor, i.e. the mass eccentricity $e = 0.01$cm, will achieve the effect of vibration depression. The calculations show that the effect of vibration depression with two squeeze-film dampers is better than that with one. This conclusion has also been proved by the measured vibration data of a jet engine.

PHOTOTHERMOELASTIC EXPERIMENTAL INVESTIGATION OF TURBINE DISK

Dong Benhan and Wang Ju

(*Shenyang Aeroengine Research Institute*)

Abstract

This paper deals with three aspects of photothermoelastic study of the steady thermal stress field on the turbine disk.

First of all, the test methods and techniques are investigated. It is necessary to select a suitable model material which will not change mechanical and optical properties within the range of test temperature. In this experiment the epoxy resin is adopted. Then, it is imperative to determine measuring and recording methods of temperature and to research heating ana controlling techniques of temperature field. In this case, the surface of outer edge of the disk is wrapped with heating tape which is a polyester film coated by carbon. The temperatures of the model are measured with thermocouples EA2 embedded in the surface or indepth of the model, and are autocontrolled.

Secondly, the photothermoelastic experiment and theoretical calculation of a plane disk have been carried out. Both results of experiment and calculation are in good agreement. It is proved that the methods and techniques proposed can be usefulfor practice.

Thirdly, the photothermoelasticity model test of a turbine disk has been completed. The data of the test can be used as a reference for turbine disk design.

OPTIMUM DESIGN FOR PROFILE CONTOUR OF TURBINE DISK

Lin Xiurong

(*Northwestern polytechnical University*)

Abstract

A combined optimization method for searching the minimum disk weight and the best disk profile contour is provided which uses the random-walk method and the random-try method alternately. The whole disk profile contour can be linearized by linear segments, and thus the disk can be treated as a series of trapezoid-section ringlets. A subroutine for automatical generation of calculation sections is deveonloped. Taking the disk weight as objective function, the geometric parameters and the axial thickness of the ringlets as design variables, and the five stress criteria as constrains, we applied the combined optimization method to a practical disk and obtained a feasible point within 5—7 minutes on an IBM-PC. After one hour calculation the disk weight has been reduced 12.22%. It is proved that this method increases convergence rate obviously.

HIGH- AND LOW-CYCLE COMBINED FATIGUE AND ITS TEST TECHNIQUE

Liang Guowei

(*Northwestern Polytechnical University*)

Abstract

A simple combined fatigue test facility is introduced, which produces and controls high- and low-frequency combined load spectra by means of a closed circuit consisting of a microcomputer and a hydraulic servo unit. The minor-cycle frequency attains 100Hz with a force amplitude of about 500kg, but higher frequency (say, 400-500Hz) may be attained if a better servo unit be available.